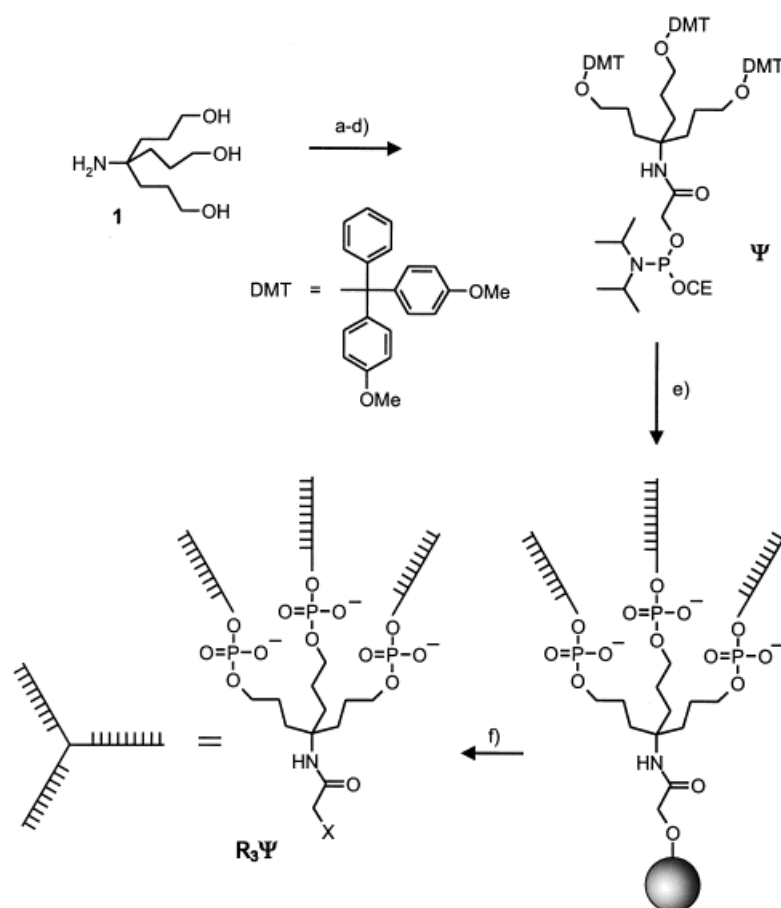


# Self-Assembly of Trisoligonucleotidyls: The Case for Nano-Acetylene and Nano-Cyclobutadiene\*\*

Matthias Scheffler, Axel Dorenbeck, Stefan Jordan, Michael Wüstefeld, and Günter von Kiedrowski\*

DNA as well as DNA-like materials enable sequence-addressed self-assembly and thus supramolecular information processing in a unique way. Since the pioneering experiments of Seeman,<sup>[1]</sup> the potential of using DNA as construction material for synthetic nanometer-sized objects has been recognized within bioorganic and supramolecular chemistry. Wire-frame-type molecular objects were synthesized from three-way or four-way junctions which are themselves composed of three or four linear oligonucleotides.<sup>[2]</sup> Recently, Shi and Bergstrom reported on the assembly of nanometer-sized macrocycles from complementary V-shaped molecules in which the 3'-ends of two oligonucleotides were attached to a bifunctional linker.<sup>[3]</sup> Further approaches within DNA nanotechnology focus on the oligonucleotide-addressed spatial positioning of molecular objects such as metal clusters that are covalently attached to single-stranded, linear oligonucleotides.<sup>[4]</sup>

We here report on the synthesis and sequence-addressed self-assembly of trisoligonucleotidyls, a novel class of branched oligonucleotides in which a trifunctional linker connects three oligonucleotide strands through their 3'-termini. Our concept of synthesizing DNA nanostructures is related to that of Seeman; it is, however, solely based on self-assembly, thus avoiding covalent ligation steps in order to enable future approaches towards the self-replication of such nanostructures. Trisoligonucleotidyls based on the linker  $\Psi$  (Scheme 1) were synthesized by solid-phase phosphoramidite chemistry as early as 1993,<sup>[5a]</sup> but the lack of proper analytical methods for the identification of these molecules prevented an early publication. Table 1 presents the sequences and selected analytical data of the trisoligonucleotidyls.<sup>[5b]</sup> Linker phosphoramidite  $\Psi$  was obtained from Newkome's dendrimer synthon **1** by a four-step transformation sequence in 50% overall yield (Scheme 1).<sup>[6]</sup>



Scheme 1. Synthesis of trisoligonucleotidyls  $R_3\Psi$ . a) 4,4'-dimethoxytrityl chloride, pyridine; b) acetoxyacetic acid chloride, triethylamine, toluene; c) 0.5N NaOH/THF (1/1); d) 2-(cyanethoxy)-bis-*N,N*-(diisopropylamino)phosphane, dichloromethane; e) standard phosphoramidite protocol for oligonucleotide synthesis on 500 Å CPG, except during coupling of  $\Psi$ , where the reaction time was extended to  $3 \times 15$  min; f)  $NH_3$  (aq) at 85°C for 2 h in a pressure-tight tube; note that under these cleavage conditions the amido functionality at the 3'-termini of the linker is not affected, so that the leader base(s) X from the solid phase is incorporated into the trisoligonucleotidyls. – CE = cyanethoxy.

UV-titration data allowed us to determine the stoichiometry of different trisoligonucleotidyl complexes. Mixtures of trisoligonucleotidyls with their linear complements showed always a 1:3 stoichiometry (Figure 1a), whereas mixtures of complementary trisoligonucleotidyls showed always a 1:1 stoichiometry (Figure 1b). The UV melting curves of complexes between complementary linear oligonucleotides and between complementary trisoligonucleotidyls as well as of the above-mentioned 1:3 complexes were barely distinguishable at concentrations adjusted to obtain equal UV extinction  $E$ .<sup>[5b]</sup> Transitions were monophasic in all cases, even when varying the heating rate between 0.1 and 2 Kmin<sup>-1</sup>. Obviously, trisoligonucleotidyls undergo self-assembly as efficiently as their linear counterparts.

The size distribution of trisoligonucleotidyl complexes was visualized by means of agarose gel electrophoresis. Immobile high molecular weight aggregates were obtained from complementary trisoligonucleotidyls when a standard hybridization protocol was employed, in which the sample is denatured at 95°C and then slowly cooled to the annealing temperature (0.1 Kmin<sup>-1</sup> to 20–25 K below  $T_m$ ). The formation of these

[\*] Prof. Dr. G. von Kiedrowski, Dr. M. Scheffler, A. Dorenbeck, M. Wüstefeld  
Lehrstuhl für Bioorganische Chemie der Universität  
D-44780 Bochum (Germany)  
Fax: (+49) 234-7094-355  
E-mail: kiedro@ernie.orch.ruhr-uni-bochum.de  
Dr. S. Jordan  
Bayer AG, 51366 Leverkusen (Germany)

[\*\*] This work has been supported by Deutsche Forschungsgemeinschaft (SFB 452) and Fonds der chemischen Industrie. We thank R. Breuckmann for help on the MALDI-MS analysis of the compounds.

Supporting information for this article is available on the WWW under <http://www.wiley-vch.de/home/angewandte/> or from the author.

Table 1. Sequence and analytical data of the trisigonucleotidyls  $\mathbf{R}_3\Psi$  (Scheme 1).<sup>[a]</sup>

$\mathbf{R}_3\Psi$ <sup>[b]</sup>	Sequence	$X$ <sup>[c]</sup>	$M_{\text{calcd}}$	$M_{\text{found}}$ <sup>[d]</sup>	$t_m$ [min] <sup>[e]</sup>	$t_r$ [min] <sup>[f]</sup>	Yield [nmol] <sup>[g]</sup>
$\mathbf{A}_3^*\mathbf{Y}$	ATTGGCGCCAAT	pTA	11990	11981.7	17.89	17.55	22.50
$\mathbf{B}_3\mathbf{Y}$	AATGCCGCCAAT	pTC	11882	11878.3	19.33	16.04	52.00
$\mathbf{C}_3\mathbf{Y}$	ATTGGCGGCATT	pTC	12068	12064.4	19.58	17.23	56.45
$\mathbf{D}_3^*\mathbf{Y}$	AATTGGCGCCAATT	pTC	13827	13833.5	20.15	17.06	34.20
$\mathbf{E}_3\mathbf{Y}$	AAATGCCGCCAAAT	pTA	13785	13780.9	20.68	16.51	33.00
$\mathbf{F}_3\mathbf{Y}$	ATTTGGCGGCATTT	pTA	13917	13929.6	21.42	17.56	53.75
$\mathbf{G}_3^*\mathbf{Y}$	ATAATGGCGCCATTAT	pTT	15679	15700.9	22.50	18.22	13.45
$\mathbf{H}_3\mathbf{Y}$	AATCAGCCGCCACAAT	pC	15192	15185.2	22.81	16.63	78.74
$\mathbf{I}_3\mathbf{Y}$	ATTGTGGCGGCTGATT	pC	15562	15554.9	23.35	16.62	86.23
$\mathbf{J}_3^*\mathbf{Y}$	ATTGGACCGCGTCCAAT	pC	17236	17238.2	–	17.40	8.20
$\mathbf{K}_3\mathbf{Y}$	AATCCTCCGCGTCCAAT	pTA	17201	17226.3	26.42	17.02	33.10
$\mathbf{L}_3\mathbf{Y}$	ATTGGACGGCGGAGGATT	pTA	17922	17938.1	24.59	17.47	27.45
$\mathbf{M}_3^*\mathbf{Y}$	ATTGGGACCGCGTCCAAT	pC	19107	19123.2	–	16.38	10.10
$\mathbf{N}_3\mathbf{Y}$	AATCCCTGCCGCCTCCAAT	pTC	18913	18926.8	29.25	16.94	24.70
$\mathbf{O}_3\mathbf{Y}$	ATTGGGAGGCGGCAGGGATT	pTC	19873	19887.7	29.37	17.89	32.70

[a] The materials were purified by denaturing polyacrylamide gel electrophoresis (PAGE, 10–16% acrylamide) followed by desalting on NAP (NAP) columns (APB). Characterization was carried out with capillary electrophoresis (CE), HPLC, and MALDI-TOF-MS. [b] An asterisk indicates a self-complementary sequence. [c] p denotes a phosphodiester linkage. [d] Determined by MALDI-TOF-MS: 3-hydroxypicolinic acid, acetonitrile/ $\text{H}_2\text{O}$  (1/1). [e]  $t_m$  is the time of migration as determined by CE on eCAP-cartidge (27 cm, 0.1M tris-borate buffer, 7M urea, 10 kV). [f]  $t_r$  is the time of retention as determined by HPLC on Lichrocart C-18 (Merck; eluent A: 0.2M triethylammonium acetate, 2% acetonitrile (pH 7); eluent B: acetonitrile; gradient: eluent A for 5 min, 0→25% eluent B within 25 min, 25→50% eluent B within 3 min). [g] Yield after purification from a 1.3- $\mu\text{mol}$  scale.

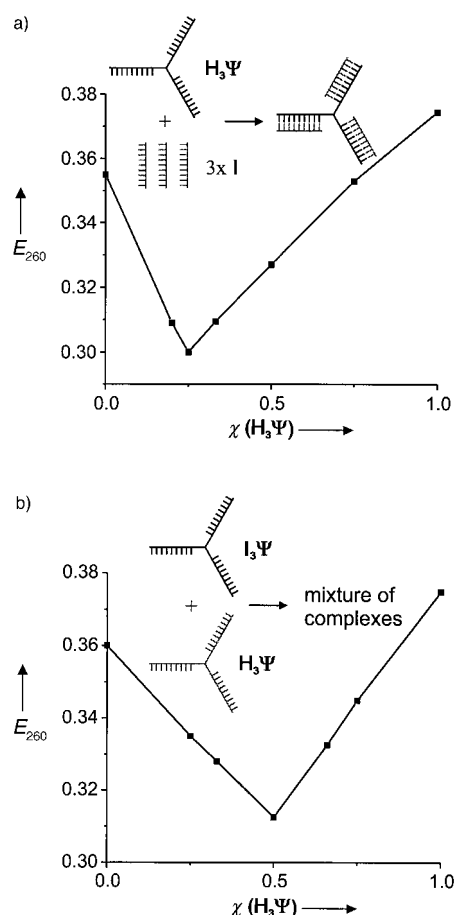


Figure 1. Determination of the stoichiometry of the trisigonucleotidyl complexes by UV-titration. The UV-extinction  $E$  at  $\lambda = 260$  nm was measured as a function of the mole fraction  $\chi$  of  $\mathbf{H}_3\Psi$ . a) Mixing curve for  $\mathbf{H}_3\Psi^*\mathbf{I}$  showing a 1:3 stoichiometry; b) mixing curve for  $\mathbf{H}_3\Psi^*\mathbf{I}_3\Psi$  revealing a 1:1 stoichiometry. All experiments were carried out under extinction equivalence in the presence of 100 mM NaCl, 0.5 mM EDTA, and 10 mM phosphate buffer (pH 7.5) and at 25 °C. The concentration of  $\mathbf{H}_3\Psi$  was 0.333  $\mu\text{M}$  at  $\chi = 1$ .

polymeric aggregates depends on the concentration of the trisigonucleotidyls and has been observed, for example, for the case  $\mathbf{H}_3\Psi/\mathbf{I}_3\Psi$  at  $c > 1$   $\mu\text{M}$ . Discretely resolved bands could, however, be made visible after changing the hybridization strategy (see the Supporting Information). The new protocol starts with denaturation at 95 °C followed by rapid cooling to 0 °C (1.8 Ks<sup>-1</sup> between 95 and 50 °C, see the Supporting Information), where the sample is maintained for 5 min. Afterwards, the sample is heated to the sequence-dependant annealing temperature. The rationale for the new hybridization strategy is to favour kinetically controlled association processes. This is comparable to a crystallization process where rapid cooling usually leads to high nucleation rates, resulting in smaller crystals.

Figure 2 shows a typical gel from a hybridization study in which the ratio between linear oligonucleotides  $\mathbf{H}$ ,  $\mathbf{I}$  and trisigonucleotides  $\mathbf{H}_3\Psi$ ,  $\mathbf{I}_3\Psi$  was varied. The composition of the samples applied to lanes 1–9 is given in Table 2. As expected, the linear duplex  $\mathbf{H}^*\mathbf{I}$  (lane 8) shows the highest mobility among the double-stranded complexes. The 1:3 complexes  $\mathbf{H}_3\Psi^*3\mathbf{I}$ , and  $\mathbf{I}_3\Psi^*3\mathbf{H}$  lead to single bands exhibiting equal mobility (lanes 6, 7). Lane 1 shows the distribution of complexes arising from a 1:1 mixture of trisigonucleotidyls  $\mathbf{H}_3\Psi$  and  $\mathbf{I}_3\Psi$ . The pattern of bands is also visible in lanes 2–5, where the relative amount of linear oligonucleotides  $\mathbf{H}$ ,  $\mathbf{I}$  increases. Basically, an overlap of the band patterns in lanes 1 and 6–8 is observed. The band having the highest mobility in lane 1 moves slightly faster than that in lanes 6 and 7, emphasizing that the underlying complex is structurally more compact than the 1:3 complexes. The latter was independently confirmed by size-exclusion chromatography (see the Supporting Information). The above-mentioned band is weakly visible for 14-mers  $\mathbf{E}_3\Psi$  and  $\mathbf{F}_3\Psi$ , but dominates in the case of 20-mers  $\mathbf{N}_3\Psi$  and  $\mathbf{O}_3\Psi$ <sup>[5b]</sup> its intensity critically depends on the presence of magnesium ions (5 mM) during hybridization (see the Supporting Information).<sup>[5b]</sup> In

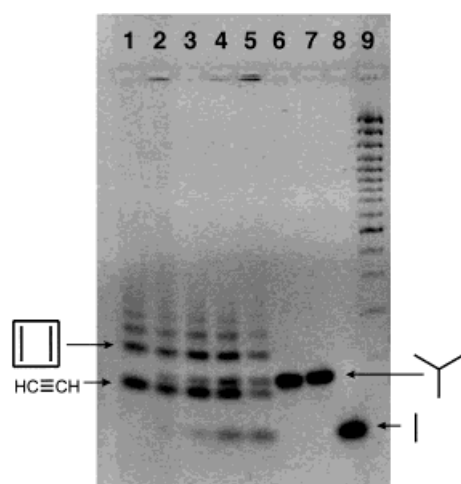


Figure 2. Oligonucleotide complexes on a 2% agarose gel (SeaKem LE; FMC) after electrophoresis and staining with ethidium bromide. The topology of the complexes is described employing hydrocarbon nomenclature as introduced in the text. The composition of the samples applied to lanes 1–9 is given in Table 2; all samples contained 100 mM NaCl, 5 mM  $\text{MgCl}_2$ , and 10 mM phosphate buffer (pH 7.5). The samples were denatured at 95 °C, cooled to 0 °C with an initial slope of  $1.8 \text{ K s}^{-1}$  and after 5 min brought to an annealing temperature of 40 °C<sup>[5b]</sup>. Electrophoresis was carried out using an ice bath for cooling.

Table 2. The composition of the samples applied to lanes 1–9 in Figure 2.

lane	$\text{H}_3\text{Y}$ [mM]	$\text{I}_3\text{Y}$ [mM]	$\text{H}$ [mM]	$\text{I}$ [mM]
1	3.33	3.33	–	–
2	3.12	3.12	0.625	0.625
3	3.00	3.00	1.75	1.75
4	2.75	2.75	1.75	1.75
5	2.50	2.50	2.50	2.50
6	–	3.33	10.00	–
7	3.33	–	–	10.00
8	–	–	10.00	10.00
9[a]	–	–	–	–

[a] Molecular weight standard: GeneRuler 100 bp DNA Ladder Plus, MBI Fermentas.

any case, the mobility data are consistent with the assumption of a bimolecular complex. Such a bimolecular complex may contain one, two, or three double-stranded linkages (Figure 3). To distinguish between the different binding situations, digestion experiments using mung-bean 5'-exonuclease were carried out (see the Supporting Information).<sup>[5b]</sup> Under conditions where single-stranded oligonucleotide **I** as well as trisiliconucleotidyl  $\text{H}_3\Psi$  were completely digested, the bands in lane 1 did not show any change, even when the reaction times were twice as long and the concentration of the enzyme was doubled.<sup>[5b]</sup> This supports the conclusion that all structures underlying the bands in lane 1 (Figure 2) are completely paired, thus removing possibilities a and b shown for the 1:1 complex in Figure 3. Further support for complete pairing was derived from scavenger experiments (see the Supporting Information). When either **H** or **I** was added to the mixture of  $\text{H}_3\Psi$  and  $\text{I}_3\Psi$  after the annealing procedure at 10 °C, no change of lane 1 (Figure 2) could be observed; that is, no single-stranded components exist in the complexes.<sup>[5b]</sup>

For the sake of simplicity, we may now introduce a simple notation for the structures under discussion. We conceive a

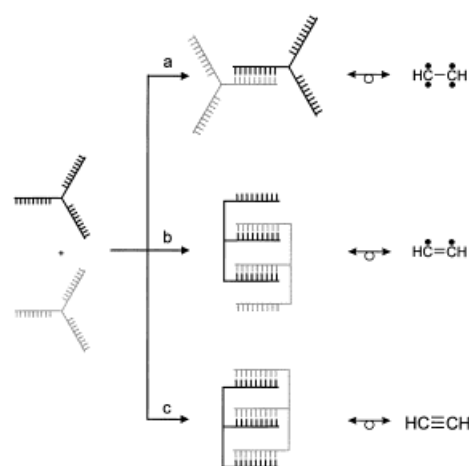


Figure 3. Possible topologies for a bimolecular complex from two complementary trisiliconucleotidyls. Each DNA double strand is described as a chemical C–C bond and each unpaired oligonucleotide as an unpaired electron.

single-stranded oligonucleotide as a free (unpaired) electron and a double-stranded oligonucleotide as a C–C bond. The complexes shown in Figure 3 may then be termed ethane-1,1,2,2-tetrayl (a), ethene-1,2-diyl (b), and acetylene (c). Complementary trisiliconucleotidyls, when processed according to the above-mentioned annealing protocol, always give rise to a series of bands whose mobilities linearly decrease with the logarithm of complex molecularity.<sup>[5b]</sup> Thus, if the band of highest mobility is assigned to nano-acetylene, the next band is consistent with nano-cyclobutadiene. Beginning with the third band, there are no longer single possibilities for the assignment of completely paired complexes, as, for example, 3:3 complexes may adopt either the topology of nano-benzene, or of nano-Dewar-benzene, or of both. Even more possibilities arise for higher complexes such as 4:4 complexes, among which nano-cubane and nano-cyclooctatetraene may exist. In any case, the first two members of the series remain rather safe to assign and are illustrated in Figure 4. Molecular modeling studies on the complex  $\text{H}_3\Psi^*\text{I}_3\Psi$  at least suggest that the case for nano-acetylene is possible, both geometrically and energetically (see the Supporting Information).



Figure 4. Models of complementary trisiliconucleotidyls (left), nano-acetylene (center), and nano-cyclobutadiene (right).

The gel of self-complementary trisiliconucleotidyls shows an alternating pattern of band intensities (Figure 5). Obviously, complexes from an even number of molecules are more highly populated than those from an odd number of mole-

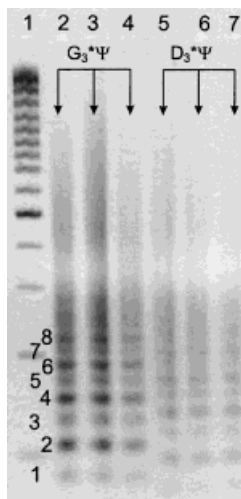


Figure 5. Agarose gel of self-complementary trisligonucleotidyls  $G_3^*\Psi$  (lanes 2, 3, 4; 3.34, 2.20, 1.67  $\mu\text{M}$ , respectively) and  $D_3^*\Psi$  (lanes 5, 6, 7; 3.34, 2.20, 1.67  $\mu\text{M}$ , respectively) after annealing in 100 mM NaCl, 5 mM  $\text{MgCl}_2$ , and 10 mM phosphate buffer (pH 7.5), following the rapid hybridization protocol for complementary trisligonucleotidyls. Bands with high intensities are assigned to fully paired complexes from an even number of trisligonucleotidyls.

cules. When comparing the intensity profiles for 14-mer and 16-mer trisligonucleotidyls,  $D_3^*\Psi$  and  $G_3^*\Psi$ , respectively (Figure 5), it becomes evident that the difference between the intensities becomes more pronounced with an increase in the chain length.<sup>[5b]</sup> Finally, self-complementary tris-18-mers  $J_3^*\Psi$  behave like mixtures of complementary tris-18-mers and show only bands for even-numbered complexes.<sup>[5b]</sup> These data again underline our previous interpretation assuming maximal interstrand pairing, which can only occur in even-numbered complexes. Self-complementary sequences may formally also exhibit intrastrand or intramolecular pairing, such as hairpins or loops. Such behaviour was considered in the design of the sequences which were selected to bear always a CG-rich central core, thus favouring interstrand pairing at the cost of intrastrand pairing. In any case, the number of pairing possibilities for such complexes exceeds that for complementary systems. As such, it is not possible to assign any binding topology, at least for the odd-numbered complexes.

We have shown that trisligonucleotidyls are suitable building blocks for the noncovalent synthesis of superstructures based on DNA double-strand linkages. Similar experiments may be carried out using DNA-based molecules that were synthesized by other linking and branching strategies.<sup>[7]</sup> Indeed, most recently, Shchepinov et al. reported a UV-melting study and claimed the formation of bimolecular complexes from complementary oligonucleotide dendrimers.<sup>[8]</sup> Nanometer-sized objects of more complex topologies and structures, even irregularly shaped, should be addressable if one starts from a multicomponent mixture of trisligonucleotidyls in which each member consists of three or more individual sequences.<sup>[5b]</sup> Those objects, when linked to other functional units, may find applications in DNA nanowiring and electronics.<sup>[9]</sup> In any case, further experiments are needed to give more detailed insight into the structure of

such nanocomplexes. As conventional spectroscopic techniques are difficult to apply for such large systems, we will report on approaches towards their direct visualization in due course.

Received: June 21, 1999 [Z13590IE]

German version: *Angew. Chem.* **1999**, *111*, 3514–3518

**Keywords:** DNA structures • hydrogen bonds • nanostructures • supramolecular chemistry

- [1] N. C. Seeman, *J. Theor. Biol.* **1982**, *99*, 237–247.
- [2] a) N. C. Seeman, Y. Zhang, J. Chen, *J. Vac. Sci. Technol.* **1994**, *12*, 1895–1903; b) N. C. Seeman, N. R. Kallenbach, *Ann. Rev. Biophys. Biomol. Struct.* **1994**, *23*, 53–86; c) C. Mao, W. Sun, N. C. Seeman, *Nature* **1997**, *386*, 3655–3662; d) N. C. Seeman, *Acc. Chem. Res.* **1997**, *30*, 357–363; e) N. C. Seeman, *Angew. Chem.* **1998**, *110*, 3408–3428; *Angew. Chem. Int. Ed.* **1998**, *37*, 3220–3238.
- [3] J. Shi, D. E. Bergstrom, *Angew. Chem.* **1997**, *109*, 70–72; *Angew. Chem. Int. Ed. Engl.* **1997**, *36*, 111–113.
- [4] a) A. P. Alivisatos, K. P. Johnsson, X. Peng, T. E. Wilson, C. J. Loweth, M. P. Bruchez, J. P. G. Schultz, *Nature* **1996**, *382*, 609–611; b) C. J. Loweth, W. B. Caldwell, X. Peng, A. P. Alivisatos, P. G. Schultz, *Angew. Chem.* **1999**, *111*, 1925–1929; *Angew. Chem. Int. Ed.* **1999**, *38*, 1808–1812; c) C. A. Mirkin, R. L. Letsinger, R. C. Mucic, J. J. Storhoff, *Nature* **1996**, *382*, 607–609; d) R. Elghanian, J. J. Storhoff, R. C. Mucic, R. L. Letsinger, C. A. Mirkin, *Science* **1997**, *277*, 1078–1080; e) J. J. Storhoff, R. Elghanian, R. C. Mucic, C. A. Mirkin, R. L. Letsinger, *J. Am. Chem. Soc.* **1998**, *120*, 1959–1964; f) R. C. Mucic, J. J. Storhoff, C. A. Mirkin, R. L. Letsinger, *J. Am. Chem. Soc.* **1998**, *120*, 12674–12675; g) C. M. Niemeyer, W. Bürger, J. Peplies, *Angew. Chem.* **1998**, *110*, 2391–2395; *Angew. Chem. Int. Ed.* **1998**, *37*, 2265–2268.
- [5] a) S. Jordan, Dissertation, Universität Göttingen, **1993**; b) M. Scheffler, Dissertation, Ruhr-Universität Bochum, Cuvillier, Göttingen, **1999**.
- [6] G. R. Newkome, C. N. Moorefield, K. J. Theriot, *J. Org. Chem.* **1988**, *53*, 5552–5554.
- [7] a) S. Teigelkamp, D. W. Will, T. Brown, J. D. Begg, *Nucleic Acids Res.* **1993**, *21*, 4651–4652; b) R. H. E. Hudson, K. Ganeshan, M. J. Damha, *Carbohydr. Modif. Antisense Res.* **1994**, *133*–152; c) R. H. E. Hudson, M. J. Damha, *J. Am. Chem. Soc.* **1993**, *115*, 2119–2124; d) M. S. Shchepinov, I. A. Udalova, A. J. Bridgman, E. M. Southern, *Nucleic Acids Res.* **1997**, *25*, 4447–4454; e) T. Horn, M. S. Urdea, *Nucleic Acids Res.* **1989**, *17*, 6959–6967.
- [8] M. S. Shchepinov, K. U. Mir, J. K. Elder, M. D. Frank-Kamenetskii, E. M. Southern, *Nucleic Acids Res.* **1999**, *27*, 3035–3041.
- [9] a) E. Braun, Y. Eichen, U. Sivan, G. Ben-Yoseph, *Nature* **1998**, *391*, 775–778; b) S. O. Kelley, J. K. Barton, *Science* **1999**, *283*, 375–381.